NUKLEONIKA 2015;60(3):683–687
doi: 10.1515/nuka-2015-0106

ORIGINAL PAPER

DE GRUYTER
OPEN

Studies of scintillator response to 60 MeV protons in a proton beam imaging system

**Marzena Rydygier,
Gabriela Mierzwińska,
Anna Czaderna,
Jan Swakoń,
Michael P. R. Waligórski**

Abstract. A Proton Beam Imaging System (ProBImS) is under development at the Institute of Nuclear Physics, Polish Academy of Sciences (IFJ PAN). The ProBImS will be used to optimize beam delivery at IFJ PAN proton therapy facilities, delivering two-dimensional distributions of beam profiles. The system consists of a scintillator, optical tract and a sensitive CCD camera which digitally records the light emitted from the proton-irradiated scintillator. The optical system, imaging data transfer and control software have already been developed. Here, we report preliminary results of an evaluation of the DuPont Hi-speed thick back screen EJ 000128 scintillator to determine its applicability in our imaging system. In order to optimize the light conversion with respect to the dose locally deposited by the proton beam in the scintillation detector, we have studied the response of the DuPont scintillator in terms of linearity of dose response, uniformity of light emission and decay rate of background light after deposition of a high dose in the scintillator. We found a linear dependence of scintillator light output vs. beam intensity by showing the intensity of the recorded images to be proportional to the dose deposited in the scintillator volume.

Key words: beam imaging • CCD camera • scintillation detector

M. Rydygier✉, G. Mierzwińska, A. Czaderna, J. Swakoń, M. P. R. Waligórski
The Henryk Niewodniczański Institute of Nuclear Physics of the Polish Academy of Sciences,
152 Radzikowskiego Str., 31-342 Krakow, Poland,
E-mail: marzena.rydygier@ifj.edu.pl

Received: 2 October 2014
Accepted: 20 May 2015

Introduction

In this study we present the results of measurements performed with the ProBImS [1], an IFJ PAN-developed, proton beam spatial beam fluence imaging system consisting of a scintillator, a charge-coupled device (CCD) camera and in-house developed and implemented data acquisition and management software. In order to consistently deliver a precisely determined radiotherapy dose to the target volume, Quality Assurance (QA) procedures need to be applied to the passively scattered proton beam applied in ocular tumor treatment at IFJ PAN [2]. These procedures include verification of the physical parameters of the proton beam. For clinical application of proton beam techniques (in passive or scanning modes), determination of depth-dose distributions and of cross-sectional beam profiles are essential [3, 4]. The new system will speed up verification and recording of pristine and spread-out proton beam parameters (i.e. dose distribution, distal fall-off), which is currently performed using a parallel-plane Markus ion chamber. The system will also allow us to improve the quality of transversal beam measurements, that is, of proton beam emittance profiles, of dose uniformity, or of lateral penumbrae at different beam ranges. Currently, all these measurements are performed using a setup with a semiconductor diode, which is an elaborate and time-consuming procedure.

Materials and methods

The ProBImS – Proton Beam Imaging System

The ProBImS has been designed to deliver on-line two-dimensional images of the lateral profiles of the proton beam [5]. The ProBImS consists of a scintillator (converting the protons in the beam to visible light pulses), a high resolution CCD camera positioned perpendicularly to the beam axis, a glass mirror reflecting the light from the scintillator to CCD camera and light-tight cover. The CCD matrix has 3362 × 2537 pixels. A single pixel on the CCD matrix (5.4 × 5.4 μm^2) corresponds to 26 × 26 μm^2 on the scintillator. The dynamic range of the CCD signal of a single pixel is 2^{16} = 65532 ADU (analog to digital units), which is the unit of the number, as readout by the CCD electronics. To avoid radiation damage to the CCD camera matrix, the camera is positioned perpendicularly to the beam axis, with light from the scintillator being reflected by a 45-degree glass mirror. The entire system is mounted inside an anodized aluminum box (black matte) to eliminate unnecessary light reflections. The general layout of the system is presented in Fig. 1.

Optical photons are focused on the CCD matrix by an optical system. Correct screen imaging has been achieved by a large-aperture lens with a focal length of 3 m. The system employs complex recording and data transfer techniques compared to the presently used beam profile scanner with a semiconductor diode. To achieve high temporal resolution the data acquisition system is based on the standard USB protocol [1].

The most critical part of ProBImS is the scintillator, as this detector should fulfill several requirements. The main requirements are: for its spectral sensitivity spectrum to match that of the CCD camera, to be of thickness not exceeding 2 mm (so as not too markedly affect the range of the proton beam), and to feature small self-absorption and high scintillation efficiency (to gather an image of sufficient intensity over a reasonably short exposure time), and to show linear response to ionizing particle energy (in order to be able to measure the proton energy fluence) [1].

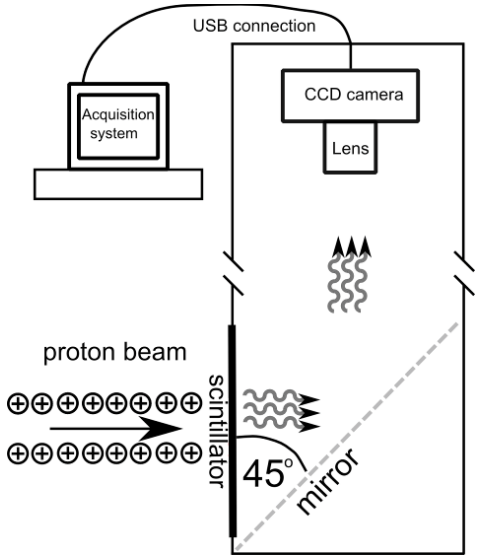

Fig. 1. Layout of the ProBImS.

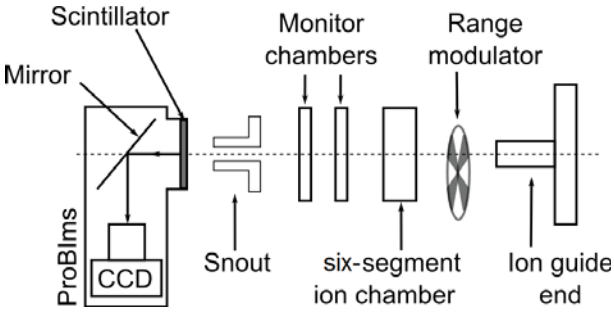

Fig. 2. Geometry of measurement using the AIC-144 cyclotron-produced proton beam. The ProBImS is positioned so as to protect the CCD camera from radiation damage from the proton beam. The beam axis is represented by the dotted line. In this figure the beam enters from the right-hand side.

The setup for measuring the scintillator response

Since many physical parameters of the proton beam need to be controlled, scintillators for the imaging system must undergo measurements under various load conditions. The DuPont Hi-speed thick back screen EJ 000128 scintillator was tested using the setup illustrated schematically in Fig. 2.

The proton beam-forming sequence consists of a single scattering foil, a range shifter and a range modulator. Additionally, a six-segment ionization chamber is used to monitor the beam direction [6]. Monitor chambers are used for dosimetry measurements. The final beam-forming elements are the snout and the end collimator. A six-segment ion chamber is used to measure the current induced by protons travelling through the segments of this chamber. While monitor ion chamber dosimetry is required in medical procedures, in this study the monitor chambers were only used to cross-check the ionization chamber measurements.

Scintillator response analysis

Lateral profiles of the proton beam can be recorded with high spatial resolution using the high-resolution CCD camera of the ProBImS. This allows the proton beam to be imaged after its formation by forming magnets, a collimator and finally by the scintillator. Unfortunately, when evaluating the proton fluence from the scintillator light emission image, proton scattering does not allow light intensity recorded by the entire CCD detector to be simply summed up. For further analysis, only the central part of the irradiated area was used. Selection of this area is necessary due to the beam intensity gradient following the beam's passage through the final collimator. This allows one to consider only the most representative uniformly irradiated part of the lateral beam profile recorded. An example of a record of the CCD camera image is presented in Fig. 3.

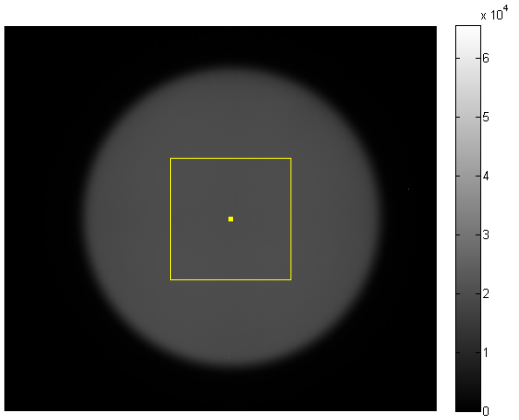

Fig. 3. Region of interest (ROI – 600 × 600 pixels) on a proton beam image recorded with ProBImS. The white dot indicates the center of gravity of the beam. The scale shows pixel intensity, in ADU.

To select the most representative region of the image (unchanged by particle scattering), the center of gravity is calculated first, according to the formula:

$$[x_C, y_C] = \left[\frac{1}{I_{\mathrm{SUM}}} \sum_{n=1}^{N} x_n \cdot I_n, \frac{1}{I_{\mathrm{SUM}}} \sum_{n=1}^{N} y_n \cdot I_n \right] \tag{1}$$

where: x_C, y_C are center of mass (image intensity) coordinates, I_{SUM} are the summed intensities of all pixels, x_n, y_n are the coordinates of n-th pixel, I_n is the n-th pixel intensity and N is the total number of pixels.

The region of interest (ROI) is an area of the image limited by a 600 × 600 pixel square, designated as:

$$\mathrm{ROI} = \left\{ [x, y] : \begin{cases} x_C - 300 \le x \le x_C + 300 \\ y_C - 300 \le y \le y_C + 300 \end{cases} \right\} \tag{2}$$

Intensity may be highly nonuniform even in the ROI, therefore to calculate the most probable intensity value and noise level (measurement uncertainty), a histogram of intensity values from ROI is calculated and plotted. A Gaussian function is fitted to the pixel intensity histogram (presented in Fig. 4), enabling one to calculate the most probable intensity value and its standard deviation, used in further analysis as an estimator of noise.

There are two separate sources of noise in visible light measurements. The first one follows from the statistical variation in the energy deposition process, related to the dose distribution. The second source is noise due to the measurement itself, namely light

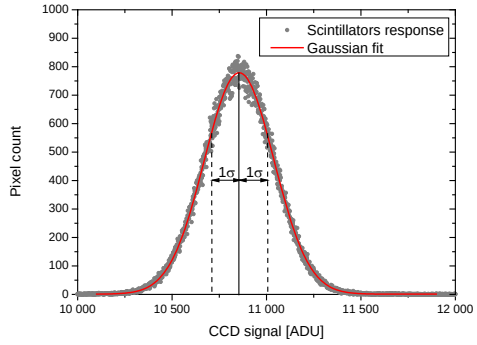

Fig. 4. Intensity histogram of the ROI of Fig. 3.

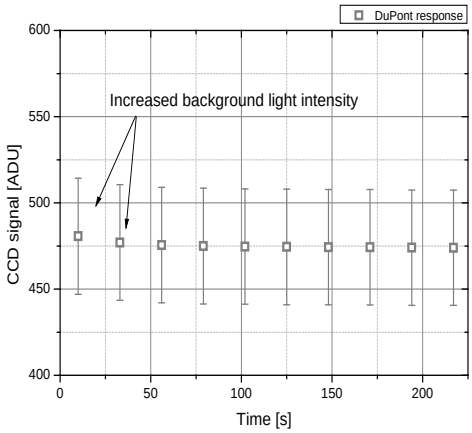

Fig. 5. DuPont response as a function of time after proton beam switch-off.

scattering inside the scintillator volume, readout electronic noise and so on. In order to determine which part of the system requires further optimization, one should identify the major sources of noise.

Intensity values presented in the next section of this paper are actually the most probable intensity values of the Gaussian fit function, as described above. The standard deviation ($\pm 1\sigma$) is represented as error bars allowing comparison of light intensity and ionizing chamber readout with an established level of confidence.

Results and discussion

Background decay rate

An important aspect of scintillator performance is its background decay rate. Measurement of the increase of background level in time after exposure of the scintillator to the proton beam is important in proton beam investigations. Scintillator activation is not observed after exposure to photon irradiation (X- or gamma-rays). To examine this property, the DuPont EJ 000128 scintillator was irradiated for 5 min by the cyclotron-produced proton beam of 20 nA current, as evaluated after its passage through the beam-forming and monitoring system. The corresponding value of absorbed dose at the isocenter of the patient irradiation facility was about 10 Gy. The first background measurement was then taken immediately after beam switch-off, with an exposure time of the CCD sensor of 10 s. The following nine measurements were taken sequentially at 13 s intervals, as required to complete the CCD readout by the analog-to-digital (ADC) converter with its exposure time set to 10 s. The DuPont scintillator showed a nearly constant optical emission level of below 500 ADU, which is very close to the noise level of CCD matrix.

In Figure 6 we present background decay measurements of the DuPont scintillator. The enhanced background light intensity over some 100 s after exposure to the proton beam most likely results from proton activation of short half-life radioactive isotopes in the scintillator. Consecutive measurements after proton beam switch-off show the background

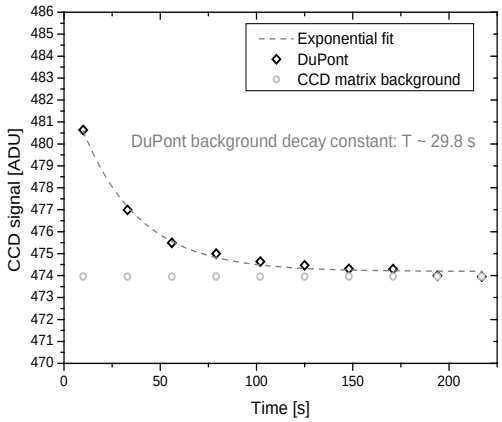

Fig. 6. DuPont scintillator background response as a function of time after proton beam switch-off.

activity of the DuPont scintillator to decay monotonically until the intensity level of an unexposed CCD sensor is reached. An overall decay half-time of 29.8 s was found by fitting an exponential function to the measured activity vs. time data for this scintillator.

It is therefore necessary to take into account enhancement of the background level of the scintillator material which may occur after extended exposure to a proton beam, due to proton activation of the scintillator material.

Scintillator intensity and dose dependence

One of the potential applications of the ProBImS is measurements of the dose distribution around the beam axis. To verify the feasibility of applying the scintillator to evaluate such dose distributions, the dose response of the DuPont scintillator was measured using a PTW Markus Type 23343 plain parallel ion chamber [7] placed at the isocenter of the treatment facility, perpendicularly to the proton beam axis, inside a PMMA phantom. The dose measurement reference setup consisted of a Markus chamber and a UNIDOS PTW T10001 electrometer [8]. Simultaneously, current measurements were taken from the monitor chambers. This allowed us to calibrate the monitor chamber response against dose, as measured by the PTW Markus chamber.

The response of the DuPont scintillator after proton irradiation within the dose range between 1 Gy and 15 Gy is presented in Fig. 7a. This series of measurements was performed in the spread-out Bragg peak region to deliver a uniform dose across the entire thickness of the scintillator. Bragg peak spreading was achieved using a range modulator to achieve full range (approx. 28.8 mm) beam modulation. Measurements were performed over the spread-out Bragg peak entrance only.

The response of the DuPont scintillator after doses of γ-rays from a Co-60 radiotherapy source is shown in Fig. 7b (note the different ranges of CCD camera response in Fig. 7a and Fig. 7b). Dose rate measurements were performed using the PTW Markus ion chamber and PTW UNIDOS electrometer set. For this purpose, a 10 cm × 10 cm collimator was used, at a SDD (source to detector distance) of ca. 50 cm. In order to account for dose build-up, a 5.3 mm thick poly(methyl methacrylate) (PMMA) plate was used to cover the scintillator.

As shown in Fig. 7, the response of the DuPont scintillator is linear with dose, after proton and gamma irradiation. Due to the lower signal-to-noise ratio in the case of gamma irradiation, higher measurement uncertainties are observed in Fig. 7b. The dose rates during gamma exposition were about 0.7 Gy/min and about 0.2 Gy/s during proton irradiation. On a per unit dose basis, the response of the DuPont scintillator after the proton beam is two times lower than that after gamma rays. The CCD signal after a proton dose of 10 Gy is about 30 000 ADU, while the same gamma-rays dose gives about 60 000 ADU. Moreover, the optical diaphragm diameter in the case of proton beam exposures was wider (1.8) than that in gamma-ray exposures (5.6), showing that the scintillator efficiency after gamma ray-exposures is even higher.

Two-dimensional spatial distribution of the proton beam

The spatial stability of the beam can be controlled on-line using our ProBImS. In Figure 8a, we show an example of a 2D distribution of proton beam fluence collected by this system using the DuPont

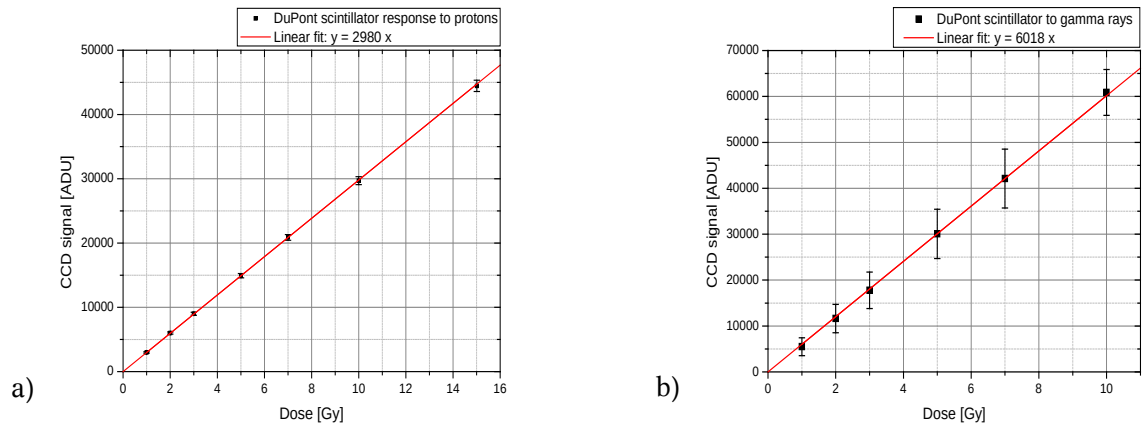

Fig. 7. Correlation between light intensity recorded with CCD camera and dose deposited in the DuPont scintillator: a) proton dose response, diaphragm setup 1.8; b) gamma-ray response, diaphragm setup 5.6.

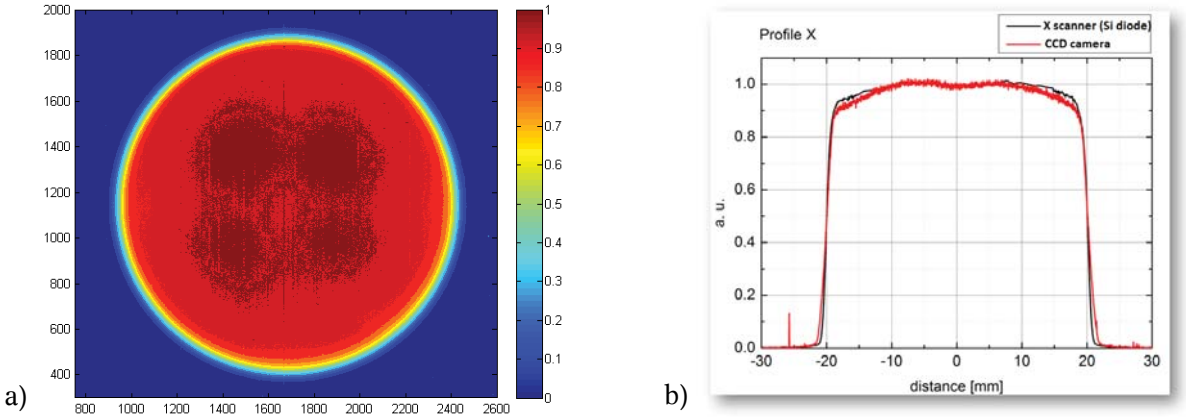

Fig. 8. Two-dimensional fluence distributions of the AIC-144 cyclotron-produced proton beam: a) image recorded with ProBImS using DuPont scintillator, b) profiles extracted from the image.

scintillator. A considerable advantage is seen of using the ProBImS for this purpose over the presently used one-dimensional X scanner and semiconductor diode setup which determines cross-section profiles only. Every 2D image recorded with our system can be decomposed into lateral profiles over any intersection plane of the beam (Fig. 8b). The set of parameters extracted from these profiles can be used to evaluate the quality of the proton beam. The results generally agree with similar beam profile measurements performed using the semiconductor diode and scanner setup, as shown in Fig. 8b.

Conclusions

To control the dose received by the patient over the whole treatment cycle, and for regulatory reasons, proton beam preparation procedures currently applied at IFJ PAN require dose monitoring with a reference ion chamber and electrometer setup, before each dose fraction is delivered to the patient's tumor volume. Continuous development of improved methods and techniques is necessary to perform proton beam imaging and dose measurements reliably and more rapidly. We believe that when fully developed, ProBImS will be used to verify the shape of the individual collimator, to assess the uniformity of irradiation of the tumor volume and to verify the dose delivered to this volume. The ability of the ProBImS to perform these elements of beam QA is a single measurement will greatly reduce the time required to prepare the proton beam for patient irradiation.

Acknowledgments. This work has been supported by The EU Human Capital Operational Program, Polish Project No. POKL.04.0101-00-434/08-00. One of the authors (MPRW) is also employed at the Centre of Oncology, Maria Skłodowska-Curie Memorial Institute, Krakow Branch, Poland.

References

1. Boberek, M., Swakoń, J., Stolarczyk, L., Olko, P., & Waligórski, M. (2014). A monitoring system for the 60 MeV radiotherapy proton beam at IFJ PAN using a scintillating screen and a CCD camera. *Rom. Rep. Phys*., *66*, 5–15.
2. Swakoń, J., Olko, P., Adamczyk, D., Cywicka-Jakiel, T., Dąbrowska, J., Dulny, B., Grzanka, L., Horwacik, T., Kajdrowicz, T., Michalec, B., Nowak, T., Ptaszkiewicz, M., Sowa, U., Stolarczyk, L., & Waligórski, M. P. R. (2010). Facility for proton radiotherapy of eye cancer at IFJ PAN in Krakow. *Radiat. Meas*., *45*(10), 1469–1471. DOI: 10.1016/j.radmeas.2010.06.020.
3. Lomax, A. J., Bohringer, T., Bolsi, A., Coray, D., Emert, F., Goitein, G., Jermann, A., Lin, S., Pedroni, E., Rutz, H., Stadelmann, O., Timmermann, B., Verwey, J., & Weber, D. C. (2004). Treatment planning and verification of proton therapy using spot scanning: Initial experiences. *Med. Phys*., *31*(11), 3150–3157. DOI: 10.1118/1.1779371.
4. Boon, S. N., Van Luijk, P., Böhringer, T., Coray, A., Lomax, A., Pedroni, E., & Schippers, J. M. (2000). Performance of a fluorescent screen and CCD camera as a two-dimensional dosimetry system for dynamic treatment techniques. *Med. Phys*., *27*(10), 2198–2208.
5. Cirrone, G. A. P., Coco, S., Cuttone, G., De Martinis, C., Giove, D., Lojacono, P. A., & Messina, R. (2004). A fast monitoring system for radiotherapeutic proton beams based on scintillating screens and a CCD camera. *IEEE Transact. Nucl. Sci*., *51*(4), 1402–1406.
6. Tulik, P. Golnik, N., Krzemiński, Ł., Swakoń, J., & Zielczyński, M. (2005). Komora jonizacyjna do kontroli jednorodności wiązki na stanowisku do protonowej terapii czerniaka gałki ocznej. In National Scientific Conference "Biocybernetics and Biomedical Engineering". Częstochowa, Poland.
7. PTW Freiburg. (1995). *Instruction manual for ionization chamber "Markus" Type 23343*. [D273.131.0/0].
8. PTW Freiburg. (2008). *UNIDOS® Universal Dosemeter. User manual*. [D196.131.00/13 en].